# 2
# Literature Review

## 2.1 INTRODUCTION

There has been extraordinary growth in wireless technologies during last decade. Cellular phones, global positioning systems (GPS) and wireless local area network (WLAN) modems are used to sell in very high volumes to worldwide markets. Recent years have also seen a trend of increasing integration of multiple components on single device. It is now relatively common for cellular handsets to be capable of operating at several different frequency bands, and for laptop computers to provide both Bluetooth and WLAN connectivity. This multi-band or multi-mode functionality requires several wireless transceivers in a single hardware device. Tunable devices are essential in a wide range of applications from modern telecommunication systems to satellite services. Frequency agile application stresses for the use of low loss and highly tunable devices to allow multi-band and multi-mode communication systems. Implementing a number of separate transceiver in a single hardware can increases the component count in a device and thus the overall cost which makes competition among suppliers. These requirements enforce considerable challenges on the current tunable circuit technologies. Phase shifters, tunable resonators, filters and delay lines are some of the important tunable passive devices [Schafranek *et al,* 2009]. All frequency agile devices consist of structures which are resonant systems and the resonant frequency of any system can be reduced to an equivalent capacitance (C) and inductance (L) circuit. The resonant frequency (*f*) is mathematically expressed in equation 2.1.

$$f\alpha \frac{1}{\sqrt{LC}} \tag{2.1}$$

From a physical point of view, changing either the C or L will realize frequency agility. The methods of changing the capacitance are much more feasible than changing the inductance. Therefore, using electronically tunable components in the RF and microwave circuitry, a considerable cost savings can be achieved. In such scenario, a single tunable component can replace several fixed components. For example, a bandpass filter with a tunable passband could substitute numerous fixed filters, or a tunable delay line could substitute a set of fixed delay lines in the network of a phased array antenna. Electronically tunable capacitors, also called varactors, can be used to manufacture reconfigurable components for RF and microwave devices.

Advances in science and technology have brought about the rapid evolution in electronic devices since the vacuum tube era. While the ever-increasing demands of down scaled dimension, enhanced functionality, and reduced cost have attracted the attention during the 20$^{th}$ century where tunability is emerging needs for contemporary electronics. Electronically tunable devices can adapt to the dynamic environment and therefore are 'smart' in a way to accommodate manufacturing fluctuations including changing user demands as well as minor deviations. This favourable feature makes it possible to decrease overall cost by reducing system complexity. A lot of research efforts and progress have been made in the area of tunable radio frequency (RF) and microwave devices. The established technology for microwave varactors is based on semiconductors, typically employing GaAs or silicon substrates. Development of varactors gave an interesting performance by easily incorporation in the

standard complementary metal oxide semiconductor (CMOS) integrated circuits. However, perovskite varactors have some important advantages over semiconductor varactors, including higher power handling, low losses and high tunability [Acikel *et al*, 2002]. Dielectric varactors were observed to have lower losses than silicon-based varactors above 10 GHz frequencies [Tombak *et* al, 2003]. Ferroelectric perovskite is of particular interest for tunable microwave devices, because of relatively low loss and high dielectric constant which can be tuned by applying electric field at microwave frequencies. The high dielectric constant provides benefit for minimising the size of components for thin film based devices, leading to higher integration. This size reduction is also useful in microwave circuits, where the dimensions of on-chip direct current blocking capacitors could be significantly reduced by employing BST as the dielectric instead of conventional $SiO_2$ or $Si_3N_4$ dielectric films. The two parameters that need to be optimised in ferroelectric perovskite thin films for microwave applications are the capacitance tunability and the *Q*-factor (the reciprocal of the loss tangent, $Q = 1/\tan\delta$), which should both be as high as possible. Many factors related to the device fabrication, including the substrate material, the substrate temperature during deposition, and residual strain in the thin films, among many others, affect the microwave properties of tunable varactors.

## 2.2 TUNABLE DEVICE TECHNOLOGIES

Tunable MW and RF devices have ability to rapidly tune the working frequency as per requirements and are referred as frequency-agile devices. This category includes voltage controlled oscillators (VCO), filters, phase shifters, and matching networks etc. The frequency band for RF and microwave devices normally considered from 20 kHz to 300 GHz. The three most frequently used technologies which are available in the commercial market are micro-electro-mechanical systems (MEMS), semiconductors and dielectric materials [Jakohy, *et al*, 2004].

### 2.2.1 Micro-electro-mechanical systems, (MEMS)

A micro-electro-mechanical system (MEMS) is a miniature structure that combines both mechanical and electrical functions. A basic MEMS switch and capacitor is shown in Figure 2.1. RF MEMS switches and capacitors are considered under the group of frequency tunable technology. The device changes its state by applying an electrostatic force from isolating condition (OFF) to conducting condition (ON). This ON state can be either capacitive – a capacitor or conductive – a switch based on the type of dielectric material. Micro fabrication process involves integrated circuit and hermitically packaging which makes MEMS devices relatively expensive. The parasitic losses associated within the packages and circuit connections impose a limitation on the operational frequency and therefore their consistency has also become a worry due to mechanical moving parts. RF MEMS varactors are slower in comparison with other varactors, however their high level of presentation is appreciable. MEMS based devices can be used as switches or varactors in tunable filters, antennas, phase shifters etc.

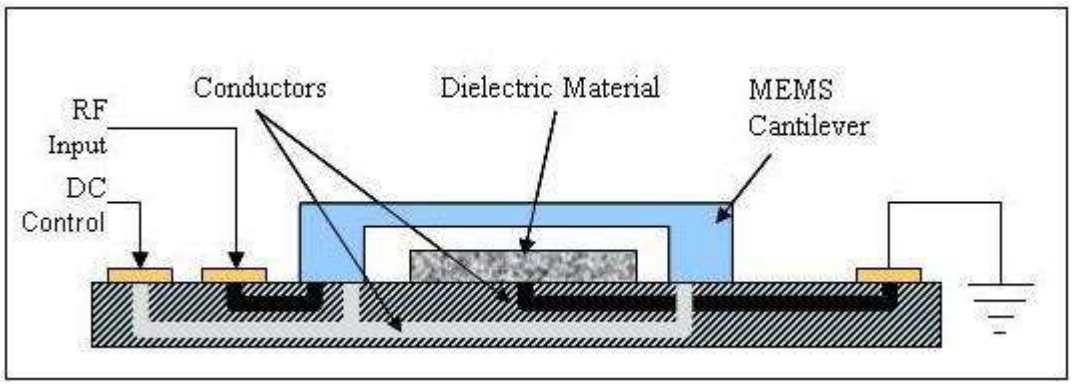


**Figure 2.1:** MEMS Tunable Capacitor (Source : http://www.memsjournal.com)

### 2.2.2 Semiconductors

The semiconductor varactor diode is very proven technology in the electronics industry. Figure 2.2 shows reversely biased PN junction to appreciate capacitance tuning. The width of depletion layer can be controlled by applying voltage. The width of depletion region grows as reverse bias voltage increases, hence the capacitance decreases and similarly by applying forward bias capacitance increases. This effect is corresponding to varying the distance between the metallic plates of a metal-insulator-metal capacitor to regulate its capacitance [Mortenson, 1974].

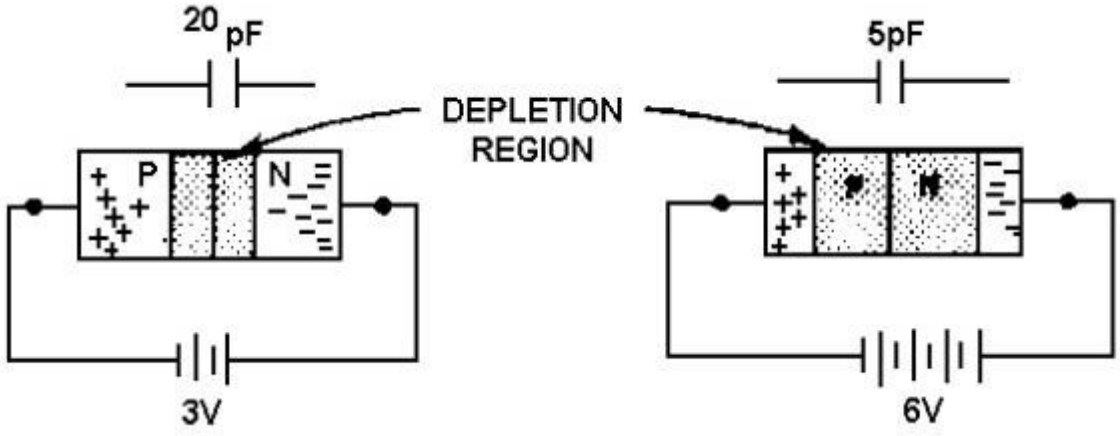


**Figure 2.2 :** Semiconductor tunable Varactor [Source http://www.slideshare.net/Enock4seth/varactor-diode]

The varactor diode demonstrate rapid and continuous tuning, however it has disadvantages in terms of lower quality factor and low power carrying capability at microwave frequencies. Presently, varactor diodes are in the application of tunable filters and Voltage Controlled Oscillators (VCOs).

### 2.2.3 Dielectric Materials

Dielectric materials commonly referred to as insulators, resist the flow of current in a circuit and can store electric charge. A material is termed as "dielectric" being its ability to store electrical energy. The ability of any two conducting plates in proximity to store a charge Q, is measured by capacitance when a potential difference V is applied across them.

$$C = \frac{Q}{V} \tag{2.2}$$

The dielectric response originated from the short-range motion of charge carriers by the influence of an externally applied field. The capacitance of a parallel plate capacitor without any dielectric in between them is known as the vacuum capacitor, whose capacitance is governed by the geometry as shown in Figure 2.3.

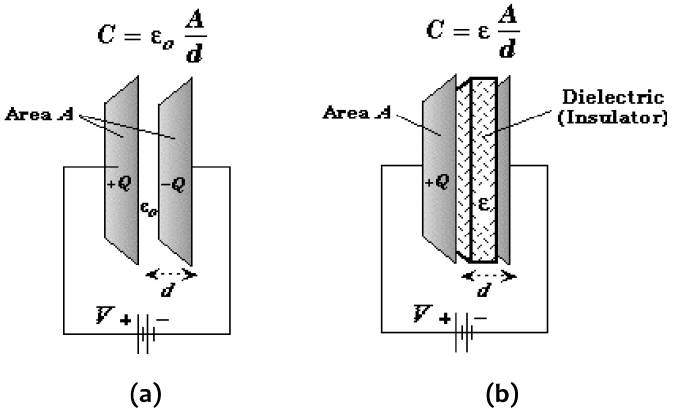


**Figure 2.3 :** Capacitance of a parallel plate capacitor with (a) vacuum and (b) dielectric material between plates.( physics-tutor.site90.net)

It is known from elementary electrostatics that charge density on the plates, Q is proportional to the area A and external electric field E. Thus the capacitance ($C_0$) of a vacuum capacitor will be as given in Eq. (2.3).

$$Q = \varepsilon_0 \frac{V}{d} A \qquad \text{and} \qquad C_0 = \varepsilon_0 \frac{A}{d} \tag{2.3}$$

where d is the distance between the plates and V is applied bias.

The proportionality constant is defined as permittivity of free space $\varepsilon_0$ ($8.854 \times 10^{-12}$ F/m). The capacitance increases with introduction of the dielectric in between the plates. The dielectric constant *k*, of the material is determined as the ratio of the capacitance 'C' of a capacitor with a dielectric medium to the capacitance '$C_0$' in vacuum between the plates.

$$\frac{C}{C_0} = k = \varepsilon_r = \frac{\varepsilon}{\varepsilon_0} \tag{2.4}$$

where ε is the permittivity of the dielectric material (F/m) . Also from the above it can be derived that dielectric constant is the ratio of the permittivity of the material to the permittivity of free space and hence it is known as the relative permittivity '$\varepsilon_r$'. When an AC sinusoidal potential $V = V_0 \exp(i\omega t)$ is applied across the dielectric medium then the charge varies according to time as shown in Figure 2.4 and the resulting current will be a combination of a charging current and a loss current which is associated to the dielectric constant.

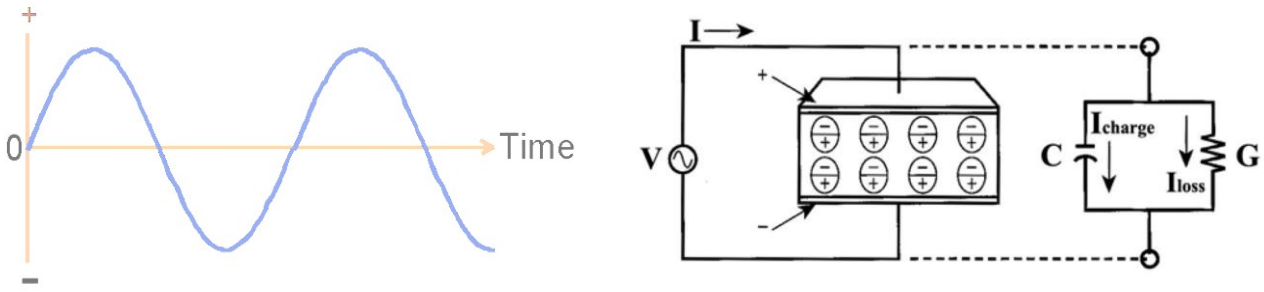


**Figure 2.4 :** AC sinusoidal potential and loss current

The loss current arises from the dissipation of energy associated with the oscillation or rotation of dipoles and long-range migration of charges, e.g., dc ohmic conduction. Another way for representation of a dielectric is use of complex dielectric constant while considering both charging and loss phenomenon to describe the material. The complex dielectric constant $\varepsilon_r$ consider a real part $\varepsilon_r'$ and an imaginary part $\varepsilon_r''$ which has significance in terms of storage and losses respectively.

$$\varepsilon_r = \varepsilon_r' - j\varepsilon_r'' \tag{2.5}$$

The real part of permittivity ($\varepsilon'_r$) indicates the energy stored in a material from an externally applied field. The imaginary part of permittivity ($\varepsilon''_r$) is associated to the loss factor and reflects dissipative nature or loosiness of the material. $\varepsilon''_r$ is always greater than zero and is usually smaller than $\varepsilon'_r$. The effects of conductivity and dielectric loss both are included in the loss factor. Figure 2.5 shows vector diagram of complex permittivity and the imaginary and real parts are shown $90^0$ out of phase. The vector sum of both the parts makes an angle "δ" with the axis of real part. The relative "lossiness" of a material is defined by the ratio of the lost energy to the stored energy.

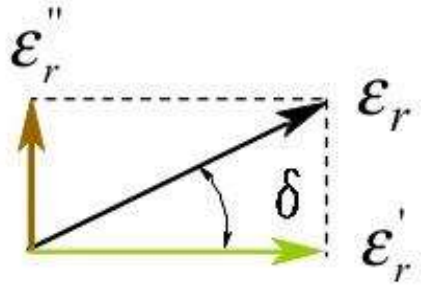


**Figure 2.5 :** Loss tangent *tan (δ)* vector scale diagram.

The loss angle, loss tangent, or tan δ is defined as the ratio of the imaginary component of the dielectric constant to the real component.

$$\tan\delta = \frac{\varepsilon_r''}{\varepsilon_r'} \tag{2.6}$$

The reciprocal of dissipation factor i.e. $(\tan\delta)^{-1}$ termed as the quality factor (Q factor) of the material, commonly utilized to define the figure of merit (FOM) in high frequency applications. It was necessity to understand the competing technologies: semiconductor varactors and ferrites to realize the capabilities of perovskite thin-film for tunable microwave technologies.

## 2.3 FREQUENCY DISPERSION IN DIELECTRICS

The dielectric material has an arrangement of charged species that can be aligned in response to an applied electric field across the material and increases the ability to store charge. The charges become polarized to compensate the electric field in such a way that the negative and positive charges move in opposite directions. The overall dielectric constant of a dielectric material may have a variety of contribution from several dielectric mechanisms or polarization effects. The frequency dependence of different polarization mechanism in dielectrics is depicted in Figure 2.6. Electronic and atomic polarisation mechanisms are comparatively weak and usually constant over the microwave region and the variation of permittivity is mainly because of dipolar relaxation in microwave frequency range. The absorption peaks in the frequency range of infrared and above is primarily due to electronic and atomic polarizations whereas the influence of ion conductivity plays role to determine ε'' in the low frequency range. The slow mechanisms drop out as frequency increases, leaving the faster ones to contribute to ε'. The magnitude of each mechanism is unique for different materials.

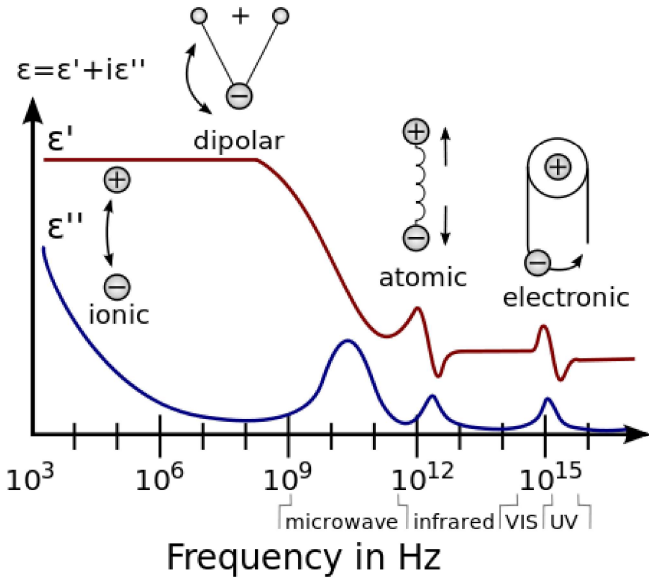


**Figure 2.6:** Frequency dependence of different polarization mechanisms
[Source : https://en.wikipedia.org/wiki/Permittivity]

### 2.3.1 Atomic polarization

By applying an external applied field, adjacent positive and negative ions stretch and give rise to atomic polarization. Ionic polarization is analogous to atomic polarization but involves the shifting of ionic species under the influence of the applied field. This shift can be significant which may lead to high values of dielectric constant, up to several thousand. The bond strength between the ions governs the frequency of resonant absorption. Atomic or ionic polarization occurs at frequencies in the infrared range i.e., about $10^{12}$-$10^{13}$ Hz.

### 2.3.2 Electronic polarization

The displacement of the electron cloud relative to the nucleus in the presence of an electric field is responsible for occurrence of electronic polarization in neutral atoms. This field induced dipolar polarisation effect used to occur in all materials, including air, but is insignificant compared to other polarization mechanisms. This polarisation mechanism is a resonant process which produces a resonance absorption peak in the UV-optical range ($10^{15}$ Hz).

### 2.3.3 Dipolar polarization

A perturbation in the thermal motion of ionic or molecular dipoles produces dipolar polarisation with a net dipolar orientation in the direction of the electric field, also referred as orientational polarization. Dipolar polarization mechanism contributes to the dielectric properties of the material in the sub-infrared range. This polarization mechanism can be conventionally classified into two categories. The molecules show a permanent dipole moment which involve rotation against an elastic restoring force with reference to equilibrium position whereas another mechanism considers the dipoles rotation between two comparable equilibrium positions. The second process is the spontaneous alignment of dipoles in one of the equilibrium positions and this is responsible to the nonlinear polarization performance along with higher dielectric constant of ferroelectric materials.

Apart from above mentioned polarisation, carrier injection becomes important at higher fields. Therefore, polarization can occur in the case of large concentration of charge carriers to form space charges at interfaces or grain boundaries because of the migration of charge carriers, designated as space charge polarization.

## 2.4 DIELECTRIC CONSTANT AND POLARIZATION

A quantitative understanding can be obtained of material's dielectric properties by establishing a relationship between the polarization 'P', in the material and its dielectric constant. The total electric displacement field D, in a dielectric caused by an external field E is the displacement $D_0$ in vacuum plus the polarization P of the material as given below in Eq. (2.7),

$$D = \varepsilon_0 E + P \qquad where, D_0 = \varepsilon_0 E \tag{2.7}$$

and defining the electric susceptibility $\chi = \frac{P}{\varepsilon_0 E}$ . The total polarisation P, includes dielectric permittivity $\varepsilon_r$ and the elemental polarizability of various charge displacement mechanisms and we have:

$$P = N_i \alpha_i E' \tag{2.8}$$

where, $N_i$ is the number of dipoles of catgory $i$ and $\alpha_i$ is the polarizability of average dipole moment per unit local field strength **E'**. The local field **E'** will be same as the external applied field **E** for simple dielectrics such as gases with small molecular interaction but polarization is substantially affected by the surrounding medium for dielectric solids.

### 2.4.1 Classification of Dielectrics

The dielectric materials can be broadly classified into two classes based on the Polarization-Electric field (P-E) characteristics i.e. linear dielectrics and non-linear dielectrics.

Linear dielectrics are the class of materials whose polarization increases linearly with increasing external electric filed and decreases to zero when the applied filed is zero as shown in Figure 2.7. These materials neither have a coercive field ($E_c$) nor saturation polarization ($P_{sat}$).

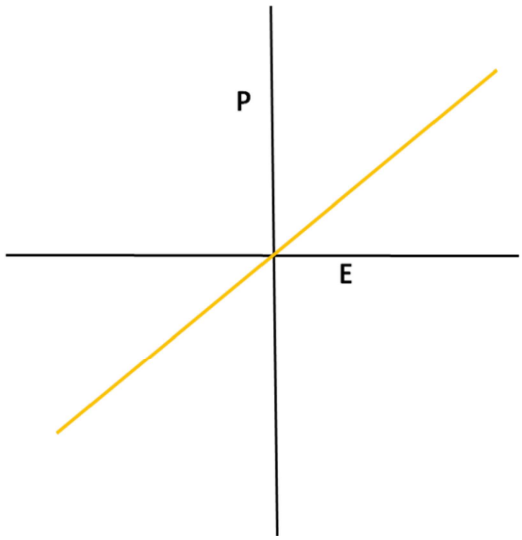


**Figure 2.7 :** P-E relationship of linear dielectrics

Nonlinear dielectrics are essentially crystalline materials which can exhibit very large value of dielectric constant. Ferroelectric materials are non-linear dielectric materials with domain configuration, hence exhibit hysteresis characteristic in polarization as shown in Figure 2.8. The electric dipoles are ordered parallel to each other in regions called domains in ferroelectric materials. These domains can switch in the presence of an external electric field from one direction of spontaneous alignment to another, giving rise to a very large change in polarization and dielectric constant.

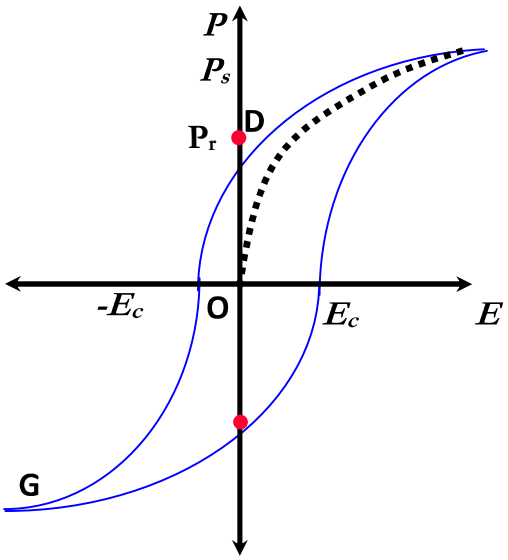


**Figure 2.8 :** Electrical polarization of nonlinear dielectrics

The nonlinear electric polarization is comparable to the nonlinear magnetic behavior of ferromagnetic materials [Moulson and Herbert, 1997]. The polarization increases with an alignment of more numbers of dipoles in the direction of the applied field when the field is initially increased from zero. When the field is increasing and strong enough to make all dipoles in alignment along the field direction, hence the material is said to be in a saturation state giving rise to a saturation polarization ($P_s$). Thereafter, the polarisation decreases from saturation with

the decreasing electric field from the saturation point. The polarization in ferroelectrics does not reach zero however the external electric field reaches zero as shown in Figure 2.8. The polarization of the material at zero field is expressed as remnant polarization ($P_r$) where ferroelectric material is still electrically polarized even in absence of external field. After applying electrical field in the reverse direction, the polarization decreases further and reaches to zero at certain value of electric field, called the coercive field ($E_c$). The coercive field is also defined as the minimum field requires to reduce the polarization of the material from its saturation to zero. The non-linear dielectric behaviour is also observed in paraelectric state of ferroelectric materials above the transition temperature. The domains contain parallel aligned electric dipoles and are separated by domain walls across which the spontaneous polarization is irregular. The $180^0$ domains are considered to have an immediate change in the polarization direction and the $90^0$ domain walls are thicker than that of the $180^0$ domain walls. The angle is the characteristic of domain walls between the directions of polarization on either side of the wall. These domain walls are formed to reduce the energy of the system.

Sodium Potassium Tartrate Tetrahydrate ($NaKC_4\ H_4O_6.4H_2O$) was the first solid, observed by Joseph Valasek in 1923, which was recognized to exhibit ferroelectric behaviour. An increase in the research occurred in 1950's on the ferroelectric materials after studies of many anomalous dielectric properties in $BaTiO_3$, leading to the extensive use of barium titanate ($BaTiO_3$) based devices in capacitor applications and piezoelectric devices. $BaTiO_3$ belongs to the perovskite family of materials. $BaTiO_3$ is the prototype of many oxides based ferroelectric perovskites which are characterized by the chemical formula as $ABO_3$. Since the discovery of ferroelectricity in $BaTiO_3$ ceramic, strontium titanate ($SrTiO_3$), barium strontium titanate ($BaSrTiO_3$), Lead titanate ($PbTiO_3$), lanthanum zirconate titanate (PLZT) and lead zirconate titanate (PZT) have been developed and utilized for a variety of applications.

The perovskite class describes a family of compounds, which all have a structure similar to $CaTiO_3$, with a general formula $ABO_3$. $CaTiO_3$ was discovered in 1839 and named after Lev Perovski. A and B are cations of different size, are usually rare-earth or transition metals in a perovskite type crystal, which are accompanied by oxygen anions as depicted in Figure 2.9. The structure can be described by a network of corner-sharing oxygen $BO_6$ octahedra in the ideal cubic case, with oxygen atoms at the faces of the unit-cell whereas A-site cations at the corner positions and the B-site cation at the center. The A-site atom has a 12-fold coordinated and B-site cation is with 6-fold coordination. In general, the perovskite are slightly distorted from the ideal cubic shape because of a non ideal relative ratio between A and B ion sizes, resulting in tetragonal or orthorhombic crystal structures. The $BO_6$ octahedra tilt or rotate in such a system, result in a lowering of the symmetry.

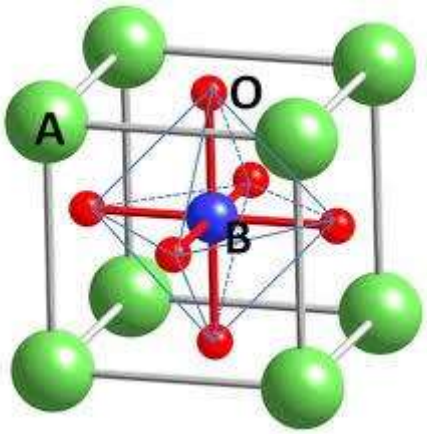


**Figure 2.9 :**$ABO_3$ perovskite structure [Source : http://www.grl.shizuoka.ac.jp/~ddsfu/Researches.html]

The widespread use of ferroelectric thin films in the areas such as capacitor applications, non volatile memories, ultrasound imaging and actuators made attraction toward research on such material. In the past few decades, many review article have been published, explaining the concepts of ferroelectricity in these materials [Mitsui *et* al, 1976]. $ABO_3$ type ferroelectric materials are non-centrosymmetric, have a unique polar axis and therefore contain electric dipoles that are spontaneously polarized, which can be reversed by application of an electric field in the opposite direction. The structural transformation from a higher to lower symmetry causes a change in the cell volume of ferroelectric material, leading to a strain in the system and hence the system exhibits domain structure in order to minimize this strain. Existence of domain structure is a hallmark of ferroelectric materials. Using tunable dielectric material, it will be sufficient in achieving variable capacitance. Utilizing bulk ferroelectric materials in tunable microwave devices was not very promising due to its low capacitance and tunability at moderate dc voltage levels. Realization of FE thin films in tunable microwave devices has been resulted in dramatic miniaturization and reduction in manufacturing cost.

It is generally recommended for microwave applications that BST thin films should be in the paraelectric phase at room temperature because of its high tunability and relatively low dielectric loss simultaneously at microwave frequencies [Tagantsev *et* al, 2003]. However, the paraelectric phase of the dielectric may not always be mandatory for tunable devices [Gevorgian *et* al, 2001]. In measurements of the high frequency tunability, it was observed that the domain wall movements do not contribute strongly at millimetre wave frequencies to microwave losses. Therefore, the paraelectric phase of BST should be used for microwave devices operating below 10 GHz, while the ferroelectric phase should be considered at higher frequencies.

Tunable dielectric films offer a excellent way of tuning into microwave circuits which was difficult to achieve with existing tuning techniques due to design issues, inadequate power handling ability, or lower Q values at the desired frequencies. Ferroelectric varactors will be prevalently used in tunable applications where the requirement of higher Q values at high frequencies and high-power handling capabilities which could not be achieved by semiconductor varactors. The most instantaneous and extensive application for tunable dielectric devices are to regulate the phase responses and frequency of microwave circuits. The key components for many tunable devices are band pass filter and phase shifter. Recent progress has been carried out for fabrication of microwave filters on dielectric substrates for its use in terrestrial and satellite applications and hence minimizes space and cost [Yamamichi *et* al, 1994]. At present, for military and satellite operations, phased array antennas are primarily used where the high cost of the antennas can be acceptable. However, ferroelectric films could provide a step forward technology to facilitate the development of low-cost phased array antennas. Moreover, the combination of moderate microwave losses, low fabrication costs and high-power carrying capabilities of ferroelectric films can effectively compete with semiconductor devices for tunable application. In general perovskite ferroelectric materials are used as capacitive layer and tunable feature of dielectric constant is helpful for tunable microwave devices. The capacitance is proportional to dielectric constant and hence it can be conveniently changed by changing applied voltage on the capacitor. The occurrence of soft mode phonon is one of the principal mechanism apart from large non linear dielectric response of the perovskite materials.

## 2.5 SOFT MODE CONCEPT AND TUNABILITY

The common and the most studied materials are barium titanate (BTO) and strontium titanate (STO) ferroelectric material in respect of theoretical as well experimental aspect. Based on extent volume effects, differences between STO and BTO were illustrated with the help of explicit first-principles calculations. This can be expressed by a dilatation of STO unit cell to the volume of BTO or the compression of BTO unit cell to the volume of STO. The $Ba^{2+}$ and $Sr^{2+}$ ion occupy the angular point sites of the unit cell corners while $O^{2-}$ occupies the face centers of the

unit cell in the case of BST. $Ti^{4+}$ forms a $TiO_6$ octahedral configuration with $Ti^{4+}$, occupying in the center of the unit cell surrounded by six oxygen $O^{2-}$ ions. The spontaneous polarization facet of ferroelectrics originated from displacement of centre of positive charges in comparison to the center of negative charge. This displacement of the $Ti^{4+}$ ion in comparison to the oxygen cage in perovskite structure, contains ionic movement same as a zone-center transverse optical (TO) phonon mode, also called "soft mode". The interplay between the local restoring force and long range dipole interaction impose low frequency of the soft mode phonon. The dielectric nonlinearity i.e. dependence of dielectric constant on the applied electric field is also based on the soft-mode behavior. The soft mode frequency hardening by introduction of applied field is the reason behind the dielectric nonlinearity in these materials [Worlock and Fleury, 1967], due to anharmonic restoring forces on the Ti ion when displaced from its equilibrium position [Rupprecht *et al*, 1961]. Higher or the field induced increase in the soft-mode frequency will lead to a decrease in the static dielectric constant according to the LST relation which is termed as "Tunability". Typically, materials with large dielectric constant have a low frequency transverse optical (TO) phonon or soft mode. The reduction of the dielectric constant with applied external field in strontium titanate thin films is a consequence of the soft-mode hardening [Sirenko, *et* al, 2000], revealed by far infrared (FIR) ellipsometry and low-frequency dielectric measurements. it has been widely acknowledged that the lattice dynamical properties in particular, the soft mode behavior is of immense importance in understanding the characteristics of such thin films where mechanism of ferroelectricity is mainly governed by lattice dynamics.

The polarisation varies non linearly with applied bias voltage or electric field. C-V profile is measure of $\Delta P/\Delta E$ where peak in C-V corresponds to large change in polarisation or ferroelectric domain switching from one orientation to another. Tunability is defined as the relative change in dielectric constant at zero bias to the dielectric constant at some non-zero bias value [DiDomenico *et* al, 1962] and expressed in Eq. (2.9) as follows:

$$Tunability = \frac{C(0) - C(V)}{C(0)} x100 = \frac{\varepsilon_r(0) - \varepsilon_r(V)}{\varepsilon_r(0)} x100 \tag{2.9}$$

where $\varepsilon_r(0)$ and $\varepsilon_r(V)$ are the dielectric constant values at zero and non-zero aaplied bias voltage/electric field respectively.

Tunable dielectric materials have a voltage-dependent dielectric constant. Majority of the applications of tunable dielectrics falls in the Radio Frequency (20 kHz to 300 MHz) and microwave (300MHz to 300GHz) circuits. The dielectric loss tangent (tan δ) or the quality factor (1/tanδ) of these materials also has electric field dependence. A major class of materials is ferroelectric that are being considered for voltage tunable applications. The loss tangent of the material is a key factor, accounted for the device performance in the development of electrically tunable devices. For practical device application, one has to carefully choose the material with optimal tradeoff between tunability and loss atngent. This can be established by using the parameter known as figure of merit (FOM), which is given as,

$$FOM = Tunability/LossTangent \tag{2.10}$$

Usually higher values of FOM is desired for voltage tunable application, where the material has high dielectric permittivity and low loss tangent. A characteristic Capacitance – Voltage (C-V) plot of ferroelectric material is shown in Figure 2.10, where it displays the characteristic "butterfly loop".

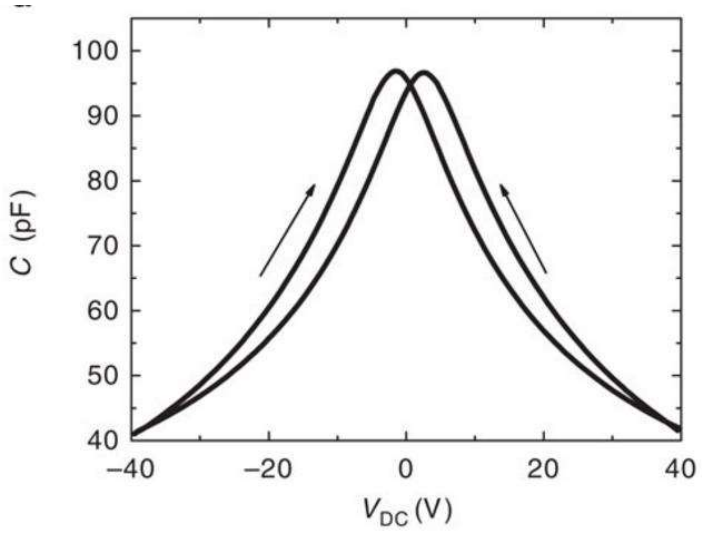


Figure 2.10 : Capacitance–voltage (C-V) 'butterfly' characteristic loop
(Source : K. Rogdakis et. al, Nature Communication 3, article 1064, 2012)

## 2.6 PEROVSKITE OXIDES FILMS FOR TUNABLE APPLICATIONS

Perovskite, ferroelectric and paraelectric, thin films have excellent dielectric properties and these properties offer its use in several capacitor applications. The important use of these high-permittivity films are as capacitor dielectric for superior packaging. In comparison to bulk, thin films can potentially applicable for higher level of integration which is a key driving force for thin-film based technologies. A tunable ferroelectric device utilizes the properties of an electrical field dependent permittivity of materials [Courrèges *et al*, 2010]. The dielectric constant or capacitance of a material can be tuned by an external applied voltage. Perovskite material thin films are feasible for practical device fabrication however bulk material exhibit the higher dielectric constant. Another reason to prefer thin-film over ceramic-chip capacitors is lower mutual inductance between the internal counter electrodes for a single layer. The thin-film devices inherently have lower inductance than multilayer capacitors. The high permittivity can be counterbalance by the thickness, if thinner films are used and result in a lower capacitance density. Moreover, leakage current level also increases with decreasing film thickness. It is important to consider low dielectric leakage because large leakage results in loss of storage charge which is undesirable for device perspective when choosing for application of tunable capacitors. Ultimately, integration of passive components as well as capacitors in the electronic systems can lead to reductions in the size and simultaneously improvements in performance of the system. Voltage dependent dielectric constant is another key property of perovskite ferroelectric thin films. Several applications for tunable devices are dependent on the capability to regulate the permittivity of the device materials. The desire to develop tuning devices have shown a path to introduce perovskite thin films as device material with low losses at microwave frequencies, low intermodulation distortion, and manufacturing cost effectiveness. Because of their advance material properties including high dielectric constant, good tunability and high breakdown voltage; perovskite ferroelectric materials, such as BST ($Ba_xSr_{1-x}TiO_3$), PZT ($PbZr_xTi_{1-x}O_3$), SBT ($SrBi_2Ta_2O_9$), etc, are being used in various RF and microwave devices [Tagantsev *et al,* 2003].

The strong interest in tunable dielectrics has been appreciated by the recent growth in microwave communications. However, the idea of using the voltage-dependent dielectric constant of ferroelectric materials like (Ba,Sr)$TiO_3$ (BST) is not new for microwave tuning applications. Difficulty to design bulk devices did not allow of making bulk ferroelectric based tunable devices that have both the low capacitances and tuning capabilities required for microwave applications. Proportionately smaller capacitance is required at higher frequencies to match the reactance of a varactor to the impedance of the rest of circuit. Therefore, the requirement to develop varactors with applicable value of capacitance for tuning at modest dc

voltage could be the reason for current emphasis on thin-film ferroelectric varactors. Ferroelectric varactors based tunable devices can be easily integrated with standard GaAs and Si processes. The performance of tunable devices governed not only by the film composition but also defects, design, strain, electrode/ferroelectric interface etc. The tunability of a BST varactor was observed greater than 40% at 25 V, in the frequency range from 1 MHz to 45 GHz which is comparable to the semiconductor analogy [Vorobiev *et al,* 2003]. Ferroelectric varactors have symmetric *C-V* characteristics. In addition, frequency independent tunability (up to 50% or more), extremely small leakage currents, dc control power, high tuning speed (< 1.0 ns) and radiation hardness are the main advantages of perovskite ferroelectric varactors. Nevertheless, ferroelectrics materials are of key interest for voltage tunable applications today. BST and PZT are frequently used perovskite ferroelectric materials because of relatively low loss, high tunability and most likely candidates to make the way in the direction of commercially available applications[Dimos and Mueller, 1998].

### 2.6.1 Barium Strontium Titanate Crystal Structure

Barium Strontium Titanate (BST) with the formula $(Ba_{1-x}, Sr_x)TiO_3$ is a solid solution of $SrTiO_3$(STO) and $BaTiO_3$(BTO). BST is a ternary compound with the type of $ABO_3$ as shown in Figure 2.11 and belongs to the perovskite family of materials. A site occupied by Ba atoms and Sr atoms and the $Ba^{2+}$ and $Sr^{2+}$ ions occupy the unit cell corners while $Ti^{4+}$ occupies the center of the unit cell. The $O^{2-}$ ions occupy the face center of the unit cell.

The titanium ion in $BaSrTiO_3$ is encircled by six oxygen ions in an octahedral configuration. The six Ti-O dipole moments cancel each other in anti-parallel pairs in a regular $TiO_6$ octahedron due to its center of symmetry. A unilateral displacement of the positively charged, $Ti^{4+}$ ion against its surrounding of negatively charged $O^{2-}$ ions which can result in net permanent dipole moment of the octahedron. Each of the oxygen is being associated with two Ti ions in the case of $BaSrTiO_3$. Consequently, the $TiO_6$ octahedra can be positioned in the same orientation at corners and fixed in location by Ba:Sr ions. This gives an opportunity for an efficient additive coupling of net dipole moment of each unit cell. Hence, this is considered as an FCC derivative structure in which the smaller Ti cation occupies the octahedral interstitial sites in the FCC array while large Ba:Sr cation and oxygen together form an FCC lattice.

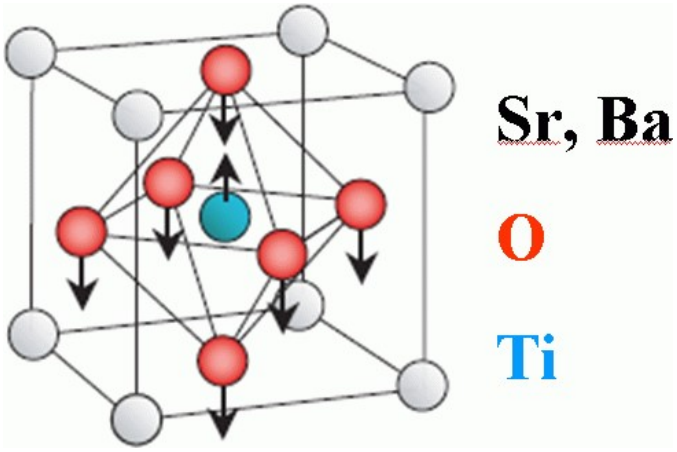


**Figure 2.11:** $BaSrTiO_3$ crystal structure; $ABO_3$ [Source : http://lts.fzu.cz/cz/res-ferro.htm]

The large size of the Ba/Sr ion increases the size of the unit cell, resulted to increase FCC Ba:Sr-O. Consequently, Ti atom is off-centered and can therefore give rise to permanent electric dipoles to achieve minimum energy positions. Above $T_c$ , the thermal energy is enough to allow the Ti ion to move at random from one position to another and hence there is no fixed asymmetry. Build up of large dipole moment by Ti atom with an applied electric field is allowed because of open octahedral site, however no spontaneous dipole alignment exists. Barium strontium titanate was widely in use as a ferroelectric tunable material for microwave

communication. Reorganization of the microscopic dipoles in a ferroelectric material on application of an external bias causes a change in the dielectric constant, which is defined as "tunability". Together with high value of dielectric tunability, the material also requires low value of loss tangent (tanδ). BST with Ba:Sr ratio of 50:50 [$(Ba_{0.5},Sr_{0.5})TiO_3$] has been considered broadly and is the composition of interest in the present study for room temperature applications. Various device technologies have employed in either bulk, thick or thin film form of BST. BST thick films requiring substantially lower tuning voltages and are considerably more practical for device applications while limited because of lower tunability for an applied voltage than that of the thin film. The most important difference is of thin film BST has been shown to have non-dispersive behavior up to 40 GHz [Demenicis *et al*, 2005]. BST thin film has been very attractive for tunable microwave devices due to the low tuning voltages, typically between 2 V to 100 V, depending on the thin-film composition, film thickness, and capacitor configuration however the dielectric loss is one order of magnitude lower for bulk BST. The properties of thin-films are invariably different compared to their bulk counterpart. The variation in capacitance with an applied bias is an intrinsic property of the material's low frequency optical phonons [Xi *et al*, 2000], not a property exclusive to thin film BST.

### 2.6.2 BST Thin Film for Tunable Application

Tunable microwave devices have considered the concept of ferroelectric films since decades. However fabrication of high-quality films can improve the requirement of practical implementation. It was demonstrated that STO films, fabricated by laser ablated method have not shown significant dispersion in dielectric constant, tan δ or tuning at higher frequencies. Epitaxial nature of the deposited film could be the reason for lack of dielectric dispersion. Measurements of highly epitaxial STO films provided substantial tuning ranges on parallel plate Au/STO/$YBa_2Cu_3O_7$ structure. The measurement on parallel-plate varactors of highly (100) oriented BST layers (0.5μm thickness) deposited by pulsed laser deposition has also showed the variation in tan δ and achieved 40% tunability with five volts dc bias at frequency of 2 GHz [Carter *et al,* 1997]. BST is considered a good material for tunable RF and microwave devices and large number of research have been carried out in aspect of device integration. MIM and IDC structures have been widely studied for their tunability and quality factor. A BST IDC with a tunability of 21% at 30V maximum bias voltage was reported [Yoon *et al,* 2003], while the fabrication difficulty of BST IDC is usually lower. Its Q factor and capacitance was measured from 17.1 to 25 and 0.78 to 0.62 pF respectively with applied bias from 0 to 30 V voltages. BST films usually have lower losses than PZT films and therefore favoured for higher-frequency applications. These BST based capacitor also reveal room temperature tuning ability and very small dispersion was observed in dielectric constant as a function of frequency. The subsequent studies of piezoelectric crystals reinforced the observation for microwave losses in association with the ferroelectricity. It was suggested that ac electric fields provides a lowest frequency (i.e. soft) mode of polarization in a forced vibration condition whereas the losses are linked with damping of the polarization by defects, impurities, or the anharmonicity of the lattice vibrations [Rupprecht, *et al,* 1961]. Virtual phonons, excited by polarisation which has frequency equal to the microwave frequency are scattered into acoustic modes, hence increasing tan δ of the material. It was also observed that room temperature losses in polycrystalline BST ceramics were dominated by scattering from the mixed (Ba, Sr) cation site. In comparison to above, losses associated with single crystal or large-grained polycrystalline STO were mainly by phonon-phonon scattering at lower temperatures due to the anharmonicity of the lattice vibrations.

There are basically two configurations of BST based capacitors i.e interdigitated(planar) capacitor and parallel plate (vertical) capacitor configuration. In parallel plate capacitor, the thin film is sandwiched between two metallic layers, also known as MIM structure. The IDC thin film is deposited directly on a substrate and the metal lines form the interdigitated structure which is deposited over the surface of the film. The device schematics for both configurations are shown in Figure 2.12.

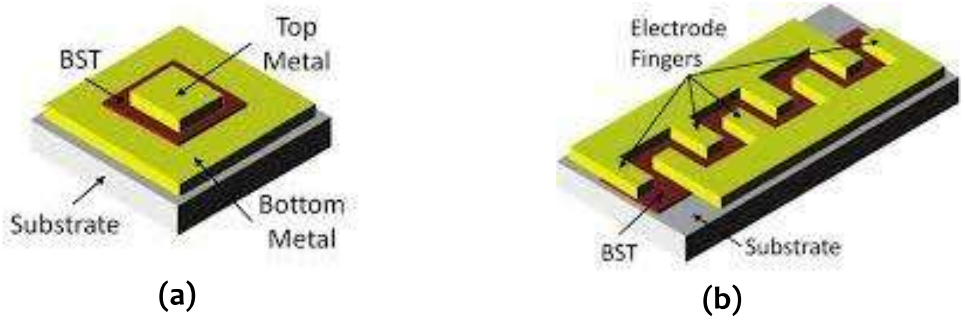


**Figure 2.12:** .Representative schematic of BST based thin film (a) parallel plate and (b) interdigitated Capacitor (Source : Acikel et al, 2002).

An interdigitated device requires a single step metallization compared to their vertical MIM counterpart and hence are simpler to fabricate and integrate into circuits. Tunability can be further increased at lower voltages by reducing spacing between the fingers. Typical operating voltages for IDCs are in the range of 0 to 100 V. Therefore, many research groups have carried out widespread research in implementing BST thin films varactors into tunable circuits like tunable filters, voltage controlled oscillator (VCO), phase shifters, tunable matching networks etc. A phase shifter using both vertical and planar varactors on sapphire and glass substrates were reported by V. Acikel *et al* [Acikel *et al,* 2001]. The voltage tunable BST based varactor demonstrated the quality factor of 29.5, associated to the higher dielectric tunability at 10 GHz frequency. The use of BST in integrated circuits on sapphire substrate was demonstrated to implement a tunable antenna. Tombak *et al* studied BST parallel plate capacitors based tunable lowpass and bandpass filters in the VHF range [Tombak *et al,* 2003]. The two parameters i.e. capacitance tunability and the *Q*-factor which should be as high as possible in BST thin films for microwave applications. Many factors related to the device fabrication, including the thin film microstructure, deposition process, surface morphology, surface states and choice of substrate material among many others influence the microwave properties of ferroelectric varactors. Therefore, it is very important to understand the relationship between the material and microwave properties of the devices in order to optimize the performance of perovskite based microwave components. However, high permittivity can only be obtained in the good microstructure which usually requires high deposition process condition. I–V characteristic of low leakage current was investigated for amorphous BST thin films after annealing at 475 $^0$C [Zhu *et al,* 2000], exhibited a characteristic insulating nature of amorphous ferroelectric materials.

### 2.6.3 Lead Zirconate Titanate structure

Lead zirconate titanate (PZT) is a member of the $ABO_3$ family of perovskites as shown in Fogure 2.13 which is thought to be a solid solution of Lead Zirconate ($PbZrO_3$) and Lead Titanate ($PbTiO_3$).

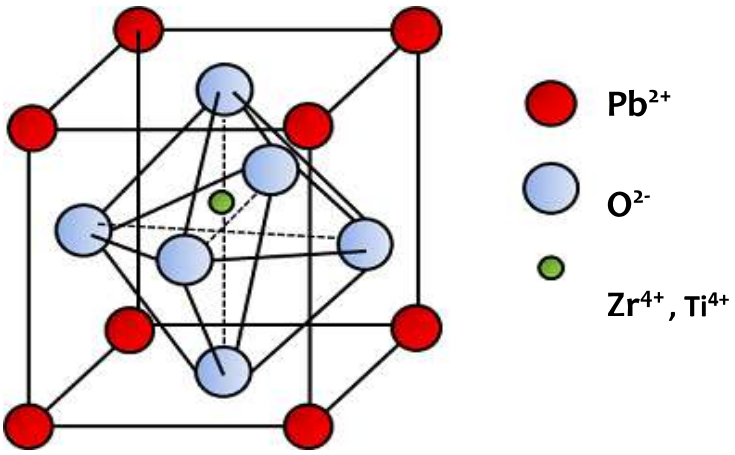


**Figure. 2.13 :** Lead zirconate titanate crystal structure

PZT exhibits both ferroelectric and piezoelectric properties and it can retain a spontaneous electric polarization where the strength of the polarization is coupled to the strain field in the crystal structure. Its chemical formula is expressed as $PbZr_xTi_{1-x}O_3$ where $x$ is the fraction of Lead Zirconate. The Pb atoms reside in the unit cell corner that is, the A sites of the perovskite structure with a $2^+$ valence state. Zr and Ti occupy B sites or the body centers and with $4^+$ valency. Oxygen atoms form the vertices of octahedra and are located on the face centers with a valence state of $2^-$. In the ferroelectric phase the structure changes from cubic to tetragonal symmetry in octahedral with Ti ion in off-centered place. These dipoles are aligned leading to a domain structure with a net spontaneous polarization with these domains.

The ferroelectric material contains regions of uniform electric polarization due to the spontaneous alignment of adjacent dipoles. Every ferroelectric domain may be oriented in any one of the possible stable directions for the particular grain orientation. The domains may be randomly oriented in the absence of an applied external electric field and overall polarization is nearly cancelled out. However, domains aligned with the electric field under the influence of applied electric field, have a lower volumetric energy density than the anti-aligned with the field. Hence, the aligned domains grow at the expense of the anti-aligned grains where domain wall motion is associated. The macroscopic polarization will retain some of the polarization even after removal of the applied field which gives rise to the polarization hysteresis as a function of applied field. The composition 52:48 of Ti:Zr is defined as morphotropic phase boundary (MPB) at room temperature. The MPB divides a tetragonal phase (Ti rich region) and a rhombohedral (the Zr rich region) ferroelectric phase. Near the composition of the MPB, an abrupt change was found in lattice constants of PZT. There is coexistence of tetragonal and the rhombohedral phases at the MPB and give rise to large dielectric constant and remnant polarization which was explained by a phase transition between the two phases [Sheen *et al,* 2003]. Polarization fatigue is the one of reason for inhibition of switchable polarization in ferroelectrics from a result of repetitive bipolar electrical pulses. Since polarization phenomenon is affected by fatigue and reduces the polarization that can be switched electrically and specifically related to the tunable applications.

### 2.6.4 PZT Thin Film for Tunable Applications

Electrical properties of Pt/PZT/ZnO/Pt capacitors, deposited by sol–gel process exhibited ferroelectric hysteresis and a voltage tunable dielectric behavior [Cagin *et al,* 2007]. The PZT films grown by a sol-gel method showed a large tunability (~60%) with low loss (tan δ = 0.028) under a relatively small bias voltage change of 40 V, could be considered further for tunable microwave applications. Lead zirconate titanate (PZT) thin films with a ration of Zr/Ti : 57/43, deposited onto bare and $RuO_2$ coated aluminium substrate showed higgh tunability and clear ferroelectric behaviour. Integrated MIM capacitors using sol-gel PZT doped with lanthanum, manganese and niobium were investigated and characterized for tunable applications. PMZT films exhibited highest tunability among the other at 100 kHz and applied bias of 20 V [Benhadjala *et al,* 2015]. The multilayer films of composition $PbZr_{0.52}Ti_{0.48}O_3/Bi_{1.5}Zn_{1.0}Nb_{1.5}O_7$ (PZT/BZN) layers have been investigated for its structural, dielectric properties and tunability [Lingxia *et al,* 2015]. Dielectric measurements of the PZT/BZN bilayer thin films exhibited low loss tangent of 0.017 and 49.7% tunability at 500 kV/cm field as shown in Figure 2.14. Lead barium zirconate (PBZ) perovskite thin films were deposited on $Pt/Ti/SiO_2/Si$ substrates and dielectric tunability of 43% was observed at 1 MHz frequency.

The radio frequency characterization of $Cu/TiN/PbZrTiO_3$ stack was performed using coplanar transmission lines and observed high dielectrcic constant along with tunability of 0.35% which suggests the use of PZT films can be well suited for tunable devices for frequencies lower than 5 GHz [Defaÿ *et al,* 2009]. Substitution of niobium for zirconium on tunable behavior enhances tunable properties of PBZ films and dielectric tunability is achieved more than 45%. Strontium modified Lead zirconate titanate ($Pb_{0.40}Sr_{0.60}Zr_{0.52}Ti_{0.48}O_3$)thin films were investigated on $Pt/TiO_2$ /$SiO_2$ /Si substrates and the films showed the figure of merit of 24 with dielectric loss of 0.02 and 48% tunability [Shao *et al,* 2006]. Moreover, the effect on the electrical properties

of $PbZrTiO_3/BiFeO_3$ (PZT/BFO) multilayers were studied and found 30% tunability at 5 V bias [Dutta, *et al,* 2012]. A gradual drop in dielectric constant and fast increase in tanδ with increasing frequency was observed during measurements on a PSZT ceramic at 0.5–2.0 GHz. The frequency dispersion in dielectric constatnt and higher losses of the PSZT sample were attributed by ferroelectric domain wall motion and such losses are intrinsic for all ferroelectric materials.

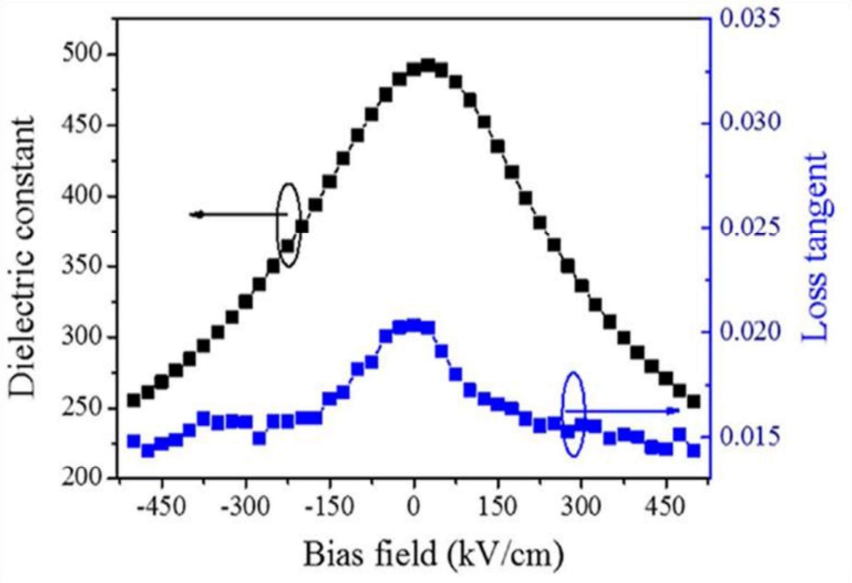


**Figure 2.14 :** Dielectric constant and loss tangent with Pt/PZT/BZN/Pt capacitors at 100 kHz.

The fatigue mechanisms by some reason are conventionally considered due to seed inhibition and domain wall pinning [Li *et al*, 2005]. A finite number of nucleation sites are formed at the interface between the electrode and the film where reversed polarization domains are nucleated. The polarization orientation has a preferred direction because of a built-in bias at the nucleation sites, can be defective regions [Tagantsev *et al,* 2001]. Non-switchable regions may also be formed due to inhibition of nucleation at some of these defective regions. These defective regions do not contribute in switching while other regions involve continously in switching which contains the same direction of polarization regardless of the applied field [Dawber *et al,* 2005]. Hence polarization is fully switched in one direction but cannot switch in the other direction during the fatigue condition. Oxygen vacancies and electronic charge carriers considered as mobile defects which can be trapped at domain walls by the domain wall pinning mechanism. The domain walls do not continue to switch and are pinned at the region where domains are surrounded by the pinning domain walls.

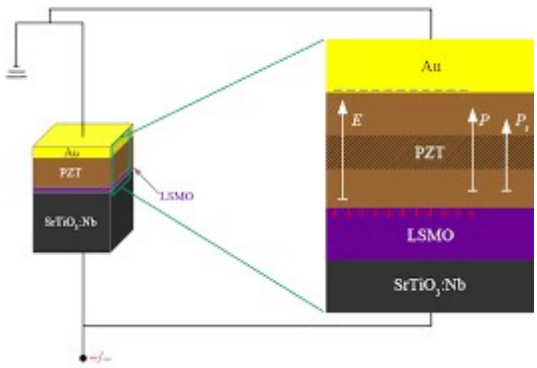


**Figure 2.15**: PZT based tunable capacitor[https://www.int.kit.edu/tunableproperties.php]

It was mentioned that electronic charge carriers were generated under thermal and optical exposure. The carriers might have trapped at domain boundaries which exhibit polarization discontinuity. The charge carrier accumulation create problem in polarization reorientation under an applied field [Daglish and Kemmitt, 2000]. The role of defects such as oxygen vacancies plays major role for polarization properties of perovskite oxides. The most commonly studied defect is oxygen vacancies [Yoo and Desu, 1992]. A distribution of oxygen vacancies close to the interface between ferroelectric and electrode was observed and then the vacancies were migrated to bulk region under a switching electric field [Schloss *et al,* 2004]. The seed inhibition and domain wall pinning mechanisms are governed by the variation in concentration and position of oxygen vacancies. Polarization fatigue is usually occurs with the result of either the injection of electrons and holes from the electrodes [Rhun *et al,* 2004] or the redistribution of oxygen vacancies into the ferroelectric thin films. The interface of ferroelectric and electrode or domain walls is favorable position for trapping of these defects.

## 2.7 HIGH ENERGY RADIATION ENVIRONMENT

### 2.7.1 Radiation in Space

On-board electronics and optoelectronic devices are designed with durability and reliability in mind while sending spacecraft and satellites into space. It is extremely difficult to repair these crafts if they are damaged while positioned in space. Radiations in space cause both temporary and permanent damage to such devices, leading to eventual operational failure. Therefore, one must understand degradation mechanisms to the operation lifetime of the device to assure its performance within acceptable parameters [Johnston *et al,* 2000]. There are three main radiation components to space radiation i.e. trapped radiation, cosmic rays and solar ares. Trapped radiation constitutes charged particles, concentrated in the Van Allen radiation belts - rings that lie in earth's orbital with a broad range of energies trapped by earth's magnetic field. Cosmic rays consist of heavy ions which may be very energetic, reaching beyond the TeV range. Primary cosmic rays originate from outside the solar system and consist of about 14% alpha, 85% protons particles and 1% heavier ions [Simpson *et al,* 1983]. Interactions between primary cosmic rays and earth's atmosphere give rise to secondary cosmic rays. Solar ares are irregular bursts of radiation originating from solar storms and consist of high fluxes of protons whereas alpha particles and electrons to a lesser extent. These cosmic rays produce cascades consisting of a variety of neutral and charged particles such as gamma photon, neutrons, mesons, muons and electrons.

### 2.7.2 Radiation in Nuclear Reactors

Intense neutron and gamma radiation fields are produced to expose the material in nuclear reactor. Proper shielding arrangements are established around nuclear reactor however electronic control systems, including communication devices implemented at various parts of a nuclear power plant, are exposed to significant doses of radiation. Many of the materials used within the electronics are highly susceptible to radiation and prone to degradation and failure over long time operation. The neutron fluxes are of the order of $10^{14}$ $cm^{-2}$ $s^{-1}$ in-core are typical for light water reactors whereas fluxes may only be as high as $10^{5}$ $cm^{-2}$ $s^{-1}$ in-containment. Furthermore, gamma dose rates vary from 10 – $10^{2}$ MGy $h^{-1}$ are present in-core and dose rates may be no higher than $10^{2}$ kGy $h^{-1}$ in containment [Holmes-Siedle and Adams, 1993]. Fast neutron fluxes still considerably lower than inside the core itself can reach $10^{9}$ cm−2 s−1; much high than the in-containment levels. An accumulated damage at these fluxes, over a period of several months to a year is adequate to affect the operability of electronic devices. The 1 MeV equivalent neutron flux at outer torus of controlled fusion reaction may vary from $10^{11}$ - $10^{16}$ $cm^{-2}$ $s^{-1}$. The use of device materials in such environments will require limitations on exposure time, careful shielding design, and the development of extremely radiation tolerant materials and technologies.

### 2.7.3 Weapons Environment for Military use

During military operation, nuclear bombs release most of their energy in the form of blast wave, nuclear and thermal radiation. An amount 15% of the total released energy is as prompt and delayed nuclear radiation in form of gamma rays and neutrons. The neutron spectrum for a fission bomb near the blast is essentially equivalent to the spectra of $^{252}Cf$ neutron source having average neutron energy of about 2 MeV while $^{60}Co$ gamma source considered equivalent to photon source. These forms of neutron and photon radiation can cause both transient and permanent effects in civilian and military electronics.

### 2.7.4 Radiation Processing Environments

In addition, many radiation processing environments are characterized by high gamma dose rates which include food, sewage and medical irradiation. These characterizations employ much higher strength (MCi) $^{60}Co$ and other strong gamma sources to sterilize or process various materials. In many phases of the high radiation reprocessing stream and in hot cells, the radiation environment is too extreme for humans, requiring the extensive use of robotics along with use of wireless communication device. The electronics in these robotic communications are prone to radiation induced degradation.

## 2.8 INTERACTION OF RADIATION WITH MATTER

There are several forms of interaction mechanism by which radiation interacts with the material in the radiation environment and can affect electronic components. The particles of the primary concern of these interactions are electrons, protons, gamma rays, neutron, alpha and beta. Radiation interaction can be categorised based on charged and uncharged particle interactions. Charged particles interaction occurs and interacts with the atomic structure during traversing in the material while uncharged particles have their interaction indirectly or by secondary radiation. The charged particle has enough energy to escape electron by ionization process. However, uncharged moving particles interact with material and lose energy by collisions or scattering. There is no direct electronic energy loss associated with neutrons due to electronic excitation and ionization. Interactions for thermal neutron are primarily elastic and inelastic scattering collisions while for high energy neutrons, non-elastic absorption reactions taken into consideration. They contribute not only to the total dissipation of the neutron's kinetic energy but also produce highly energetic secondary radiation. High energy heavy charged particles dissipate the majority of their energy through electronic processes. Uncharged particles, gamma and neutron which are of interest due its more penetration depth and give rise to produce radiation induced micro structural defect in devices.

### 2.8.1 Gamma Radiation

Gamma radiation has nature of electromagnetic waves and their interactions in the matter are different from interaction of charged particle. Electromagnetic waves have properties like particle, demonstrated with discrete levels of energy, called photons. High energy photons include gamma rays and x-rays. Gamma photons have a typical energy, determined by photon frequency. A photon can lose its energy by various mechanisms which include mainly Photoelectric Effect, Compton Scattering and Pair Production [Knoll, 2010]. The photon energy governs the probability for the occurrence of particular interaction which takes place in the matter. When gamma photon energy is less than 50 keV, gives higher interaction probability via photoelectric effect. With increasing photon energy, between 50 keV and 20 MeV, interaction via Compton scattering mechanism plays important role. Finally pair production may occur after certain threshold energy of gamma photon greater than 1.02 MeV.

#### *2.8.1.1 Photo-Electric Effect*

The gamma photon incident on matter with energy greater than the binding energy of electron then electron absorbs the energy and can be ejected from an atom. The photon is absorbed where part of energy absorbed to eject out the electron from the atom and rest of

energies carried by the electron in form of kinetic energy. This process is called as Photoelectric Effect, shown in Figure 2.16.

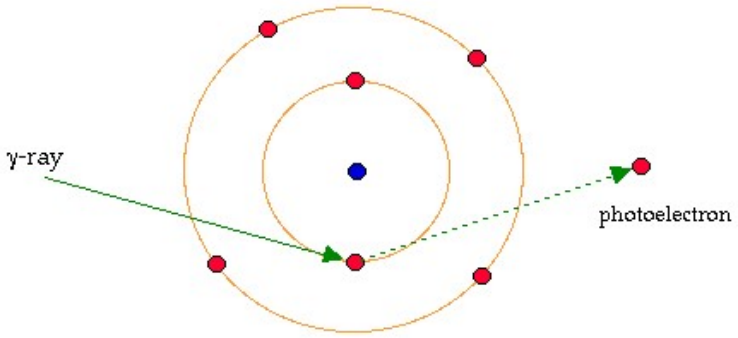


**Figure 2.16 :** Schematic illustration of photon induced photo electric effect [http://www.thefullwiki.org/Basic_Physics_of_Nuclear_Medicine/Interaction_of_Radiation_with_Matter]

The maximum kinetic energy of the electron is calculated as

$$K.E = h\nu - \varphi \tag{2.11}$$

Where $\varphi_0 = h\nu_0$ is the threshold energy which is required to eject an electron from the atom. The numbers of ejected electrons are relative to the incident gamma energy.

#### *2.8.1.2 Compton Scattering*

During the interaction of gamma photon in the matter, the photon may get scattered with the interaction with electron when the gamma photon has higher energy than binding energy of the electron.

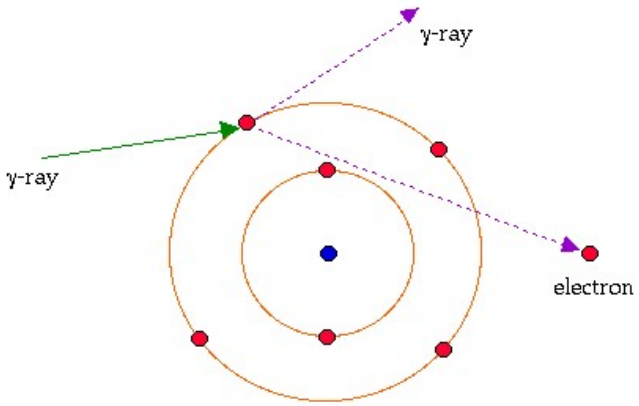


**Figure 2.17 :** Schematic illustration of Compton scattering [http://www.thefullwiki.org/Basic_Physics_of_Nuclear_Medicine/Interaction_of_Radiation_with_Matter].

The electrons get ejected from its orbital which is considered as loosely bound and the photon interaction with the loosely bound electron is expressed as Compton scattering as represented in Figure 2.17. In the Compton scattering phenomenon, the electron carries part of photon energy and gets recoils when gamma photon of energy 'hν' collides with the atom. The remaining energy is with scattered photon referred as $h\nu' < h\nu$. Also, photon scatters with an angle θ after the Compton scattering by giving a part of energy to the loosely bound electron. Therefore, the energy of the scattered photon is lesser than the energy of incident photon. The energy transfer can be explained by the principle of energy and momentum conservation.

### 2.9.1.3 *Pair Production*

A photon of energy greater than 1.02 MeV is incident on matter, interacts with the nucleus, in turn result into an electron-positron pair. This interaction process of Pair Production is illustrated in Figure 2.18. For a pair production process to occur, a photon must has a minimum threshold energy 1.02 MeV, which is nothing but the rest mass energy of two electrons.

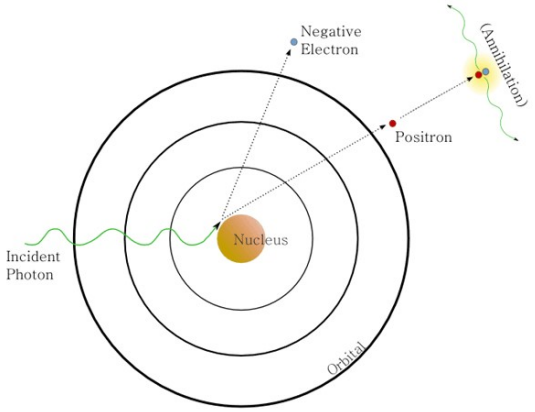


**Figure 2.18:** Schematic illustration of pair production process
[Source : https://www.med-ed.virginia.edu/courses/rad/radbiol/01physics/phys-03-05.html]

## 2.8.2 Neutron Radiation

Neutrons are uncharged particles and do not interact with atomic electrons during its passage in the material, but they do interact with the nuclei. The nuclear force is short ranged which leads to these interactions therefore, neutrons have to traverse close to nucleus for their interaction. There is low probability of interaction of the neutron, due to the small size of the nucleus, and could travel large distances in matter. There are three important neutron interaction mechanisms to produce various effects in materials i.e. inelastic scattering, elastic scattering & radiative capture.

In the case of inelastic scattering, a compound nucleus can be formed when a neutron strike to nucleus. This nucleus may emit a neutron of lower energy in association of a gamma photon which carry the remaining part of energy. The inelastic scattering is mainly effective in heavy materials and at high neutron energies while elastic scattering becomes more important phenomenon for energy loss for light nuclei and lower energies. Elastic scattering of the neutrons is similar to a billiard ball type of collision. Target nucleus receives the energy from the incident neutron and moves away at an increased speed. The collision of neutron occurs with a nucleus and rebounds in an altered direction. The neutron rebounds with almost the equal speed and little energy lose when the neutron collides with a massive nucleus. Light nuclei, on the other hand, considered more effective for slowing down neutrons which will gain a more energy during such collision.

There is possibility that neutron may get captured by the nucleus in the material. The captured nucleus will emit gamma photon. The product nuclei of (n, gamma) reactions are generally radioactive which emit gamma and beta radiation, therefore secondary radiations are produced by radiative capture process.

## 2.9 RADIATION DOSE

Radiation dose is a measure of deposited energy from the ionizing radiation per unit mass of the material. The dose is represented as radiation absorbed dose because of material dependent energy deposition. The dose units are generally mentioned in terms of radiation absorbed dose (rad) or Gray. The Rad is represented in units of erg/g and belongs to dose unit in CGS system. However, the Gray (Gy) pertains to basic dose unit of MKS system and

expressed in terms of J/kg [Knoll, 2010]. In addition to the energy and dose, flux is important unit to express the amount of irradiation. The amount of flows through a unit area per unit time is measured as flux. Particle flow is defined in terms of flux as particle $cm^{-2}$ $s^{-1}$ while this quantity is expressed by fluence and given as particle $cm^{-2}$.

## 2.10 HIGH ENERGY RADIATION EFFECTS

Wide ranges of radiation induced phenomena have been explained in many types of solids. Radiation effects contain variety of changes in macroscopic and microscopic material properties upon exposure to ionizing radiation. However, some phenomenons are unique to a particular solid and depend on its composition, structure, physical dimensions, etc. Radiation effects as a convenience are classified into two categories i.e. ionization effects and displacement effects. Ionization effects relate to the re-distribution of electrons within the solid while displacement effects are relevant to the properties related to the arrangement of atoms within a structure.

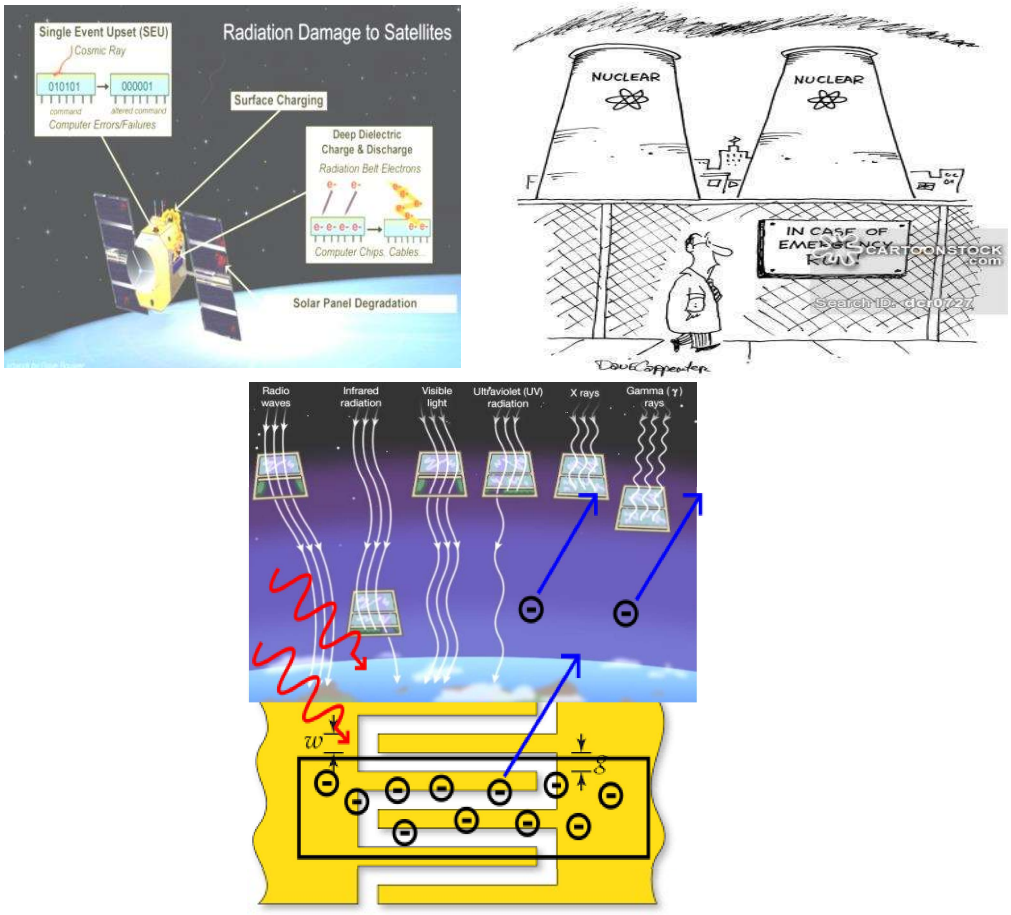


**Figure 2.19 :** Representation of radiation environment and exposure to electronic device

Due to relatively large concentrations of conduction electrons, materials with metallic bonding typically do not exhibit sensitivity to ionizing radiation. On the other hand, semiconductor and insulating materials are strongly affected by ionizing radiation with various mechanisms that lead to either enhanced or suppressed defect accumulation. Some materials such as alkali halides, quartz, and organic materials, are susceptible to displacement damage from radiolysis reactions [Itoh and Stoneham, 2001]. In materials that are not susceptible to radiolysis, significant effects from ionizing radiation can still occur via modifications in point defect migration behavior. Substantial reductions in energy of point defect migration due to ionization effects have been predicted, and significant microstructural changes attributed to ionization effects, observed in several semiconductors and insulator materials [Bourgoin, 1989]. The dose dependence for accumulation of the amorphous volume fraction is significantly

different for the direct impact mechanism compared to point defect accumulation or multiple overlap mechanisms [Weber, 2000]. Also the radiation dose to induce amorphisation typically increases rapidly with increasing temperature until a temperature is reached where it is not possible to induce amorphisation.

The radiation damage occurs when an incident particle dissipates its energy in the material in form of electronic and nuclear interactions. The energy dissipated by a charged particle along its trajectory as it slows down, refereed as stopping power. These energy dissipation accounts for energy loss in the form of kinetic energy transfer to nuclear matter and energy loss due to electronic excitation and ionization which are classified as nuclear stopping and electron stopping respectively. Incident high energy radiation losses its energy to ionization results in electron-hole generation in the irradiated material while non-ionizing energy loss can produce phonon and displacement of atoms in the lattice. In general, the initially created defects are vacancies and interstitials. An interstitial atom is dislodged and resides on a non-lattice position while absence of an atom from its regular lattice position is referred as vacancy. A vacancy and a nearby interstitial are called as a Frenkel pair. A common defect is the di-vacancy which contains two nearby vacancies, created in semiconductors and insulators. Electron-hole pairs would also be generated during irradiation of devices with high energy photon in dielectric materials. There is possibility to recombine part of the electrons and holes and the rest electron-hole can disperse and transport through the matter under the applied voltage. The devices performance would degrade gradually with increasing irradiation dose and device failure can happen at higher dose due to phenomenon of total dose effect. $^{60}$Co gamma ray is a type of ionizing radiation with the average energy of 1.25 MeV which interacts with the matter with different mechanism as discussed earlier. The amount of dissipated energy depends on the composition of the material as well as the mass and charge of the incident radiation. Neutrons disperse their energy in the form of neutron-nuclear collisions. Neutron and gamma exposure can induce substantial changes in the microstructure of the materials, which are finally manifested in form of observable variation in the material's mechanical, physical and electrical properties.

### 2.10.1 Point Defects

Point defects are defined as missing of an atom or reside at an irregular position in the lattice structure. There are interstitial atoms, substitutional atoms and vacancies are class of point defects. Point defects occur around a single lattice point and do not spread in any other direction. These defects considers at most a few lost or extra atoms, however no strict limits are usually defined on dimension of point defect. From literature, many point defects, particularly in ionic crystals, are called color centers. These defects in an ordered crystal structure are typically considered as dislocation. These dislocations lead to electrochemical reactions with ionic transport through crystals.

The vacancy moves in opposite direction to the site, if a neighbouring atom moves to occupy the vacant site, and moving atom will occupy the vacant site. The neighbouring atoms will not collapse around the vacancy because of structural stability of the surrounding crystal. An attraction of surroundings atoms forces the atoms to move away from a vacancy in some materials. A vacancy or pair of vacancies is occasionally called a Schottky defect. The defects site in crystal where usually not an atom is occupied by another atom in the crystal structure, called interstitial defects. The production of defects can also be attributed by moving of an ion into an interstitial site which are usually high energy configurations. Interstitial impurity atoms are smaller in the size than the atoms and can take position between the empty space of bulk of the lattice structure. In the case of an external entity either impurity atom or high energy irradiation may be introduced in the regular lattice. Introduction of impurity atom on lattice site which is neither a vacant site nor interstitial site, called a substitutional defect. Defect complexes can be formed between different kinds of point defects depending upon the effects of external impact either from high energy radiation or else. Irradiation of any material by energetic particles leads to the displacement of an atom into an interstitial position which creates a vacancy, in turn form Frenkel defect [Hayes and Stoneham, 1985]. This could lead to formation

of three kinds of Frenkel defect pairs in the oxygen sublattice. These comprise a neutral interstitial atom and vacancy, or a vacancy along with trapped electrons and their complementary oxygen defects. The defects in oxides were studied, including $Al_2O_3$, $TiO_2$, $ZrO_2$ and the ternary oxide [Kotomin and Popov, 1998]. Electron defects were observed under electron irradiation in various perovskites $BaTiO_3$, $LiNbO_3$ and $KNbO_3$ [Hodgson *et al,* 1990]. It was reported that a local energy level, positioned 0.6 eV above the top of valence band by generation of F center in $KNbO_3$. Therefore, displacement effects come from the quasi-permanent displacement of atoms from their equilibrium positions while ionization effects result from the separation of orbital electrons from their host atoms [Lindstrom, 2003].

### 2.10.2 Microstructural Defects

At the atomic scale, the incident radiation transfers sufficient kinetic energy to an atom within the solid to displace it from its crystallographic location. Displacements are not possible below a definite energy called the displacement energy where the energy transferred is lower than the binding energy of the atom within its equilibrium site. The transfer of energy below displacement energy results in the excitation of phonons which gives collective oscillations of structure. The first displaced atom is called the primary knock-on atom (PKA). The PKA possesses additional kinetic energy in excess of the displacement energy and possibility exists that it may initiate the displacement of neighboring atoms resulting in the formation of secondary knock-on atoms (SKAs). The SKAs may give rise to additional knock-ons and so forth which forms displacement cascade. The size and energy density of the cascade volume is restricted by the incident particle type and its energy. Gamma rays experience nuclear stopping through small energy transfers, a little above the displacement energy and accumulated displacement damage primarily consists of isolated Frenkel pairs (vacancy- interstitial pairs). Cascades are unlikely to form in gamma irradiation because the majority of the PKA's energy is consumed in its formation whereas small energy is available for the creation of SKAs. Fast neutrons on the other hand, can produce high energy PKAs and by extension, large displacement cascades.

The binding energy is responsible for formation of the crystalline lattice and displacement of an atom from its lattice site requires transfer of certain minimum kinetic energy to an atom, called displacement threshold energy ($E_d$). The point defect in the lattice including an interstitial or interstitial atom can be created when an atom receives energy greater than $E_d$, which is transported from its original lattice site and reaches to rest within the lattice interstices. Isolated Frenkel pairs have the vacancy and interstitial pair, either will undergo immediate recombination or they will thermally diffuse away from one another. The cascades result in both a variety of mobile and immobile defect clusters as well as concentrated plumes of point defects while isolated Frenkel pair generate a nearly spatially uniform source of point defects and zero in-cascade clustering. Small defects in electronic materials can play a dominating role and increases in concentrations of point defects and point defect complexes which leads to significant impact on charge carrier scattering and trapping.

High energy ions, either produced from an external radiation source - such as cosmic rays or internally from PKAs and SKAs, dissipate a large fraction of their energy through the electronic stopping process of ionization. The ionization effects in metals are of zero for practical consequence due to dissipation of excitation energy in the form of heat. In semiconductors and insulators, a finite band gap separates electron hole pairs and associated with finite recombination time. The injection of an excess of holes and electrons via ionization increases the conductivity in both materials which is known as radiation induced conductivity. The presence of radiation induced structural defects produce interband energy levels which act as traps for charge carriers and generation & recombination sites. These traps are categorized as shallow levels or deep levels according to their proximity to either band edge. The shallow levels are near the conduction and valence band edges while deep levels are found near mid of the band. Shallow levels influence charge transfer time and mobility whereas deep level traps alter the recombination and creation rates for holes and electrons. The band gap in semiconductors is of the order of an eV, where recombination is fast and ionization damage is a

transient condition. For the case of insulator, recombination is a slow process due to large band gap. Therefore quasi-permanent space charges are generated from shallow trap charge carriers for long periods of time. However technically a transient condition occur by ionization effects in insulators, may persist for years or even decades. Hence both ionization and displacement effects are significant contributors to the permanent radiation effects in insulators and ceramics.

Irradiation of materials with high energetic particles can induce significant microstructural modification from crystalline-to-amorphous phase transformation. Physical and mechanical properties are governed by these microstructural changes and causes significant changes in the irradiated material. Reviews on the microstructural changes have been carried out in alloys [Kiritani, (1997], and ceramic [Zinkle, 1994] materials associated with irradiation by electrons, neutrons or heavy ions in past years. Radiation-induced amorphisation can occur by several different mechanisms, including direct amorphisation and gradual accumulation of lattice defects and chemical disorder [Weber, 2000]. Crystalline to amorphous transition has been revealed in microstructure in ion-irradiated SiC, where the amorphisation is induced by gradual buildup of radiation defects [Snead *et al,* 1998]. Direct amorphisation has been observed within individual displacement cascades in several semiconductor and insulator materials [Wang *et al,* 2001]. In many other materials, extensive chemical disordering from radiation which produces point defects precedes amorphization. Internal interfaces such as grain boundaries also play an important role in radiation induced mechanism, depending on the complexity of the microstructure. The grain boundaries generally work as sink for the point defects in the material and may play a significant role in radiation-induced microstructural changes. There has been extensive interest for use of high sink strength of nanograined materials which could lead to recombination of point defect and improved radiation resistance.

## 2.11 REVIEW OF RADIATION EFFECTS ON ELECTRONIC DEVICES

Total dose radiation effects of ionizing radiation degrade a CMOS integrated circuit by producing electron hole pairs in the gate and isolation dielectrics. The primary effects of ionizing dose on devices include charge accumulation in the oxide and interface. The electron hole pairs will be separated by the oxide electric field [McLean and Oldham, 1987]. Electrons have a relatively high mobility in oxides and swept faster at typical device operating conditions whereas holes transport slowly toward the interface via defect sites in the oxide. The electron injected from the device will make few of the holes to recombine with the electrons and other holes can form oxide trapped charge by trapping in the oxide materials. These oxide trapped charges will induce a shift in the threshold voltage and an increase in the leakage current of electrical devices. Trapping of holes and electron have been observed in some high-κ films after exposure to ionizing radiation [Felix *et al,* 2004] and significant C-V shift due to oxide trapped charges. The change of interface traps in the upper half of the silicon band gap behave like acceptor while donor like behavior in the lower half of the silicon band gap. Total dose effect of gamma-ray irradiation is the most considerable reason for irradiation induced failure of oxide devices. Generation of excess electron-hole pairs by gamma-ray irradiation and these pairs move inside the gate dielectric under the applied voltage which in turn produces oxide and interface trapped charges in the dielectric film. Singh *et al* studied the effects of heavy-ion irradiation on the electrical properties of $HfO_2$ thin films and radiation induced changes in microstructure and dielectric properties were attributed by the change in oxide and interface trap charge densities [Singh *et al*, 2012]. The effect of gamma-radiation on various high-k materials was studied by Zhao *et al* and observed radiation induced defects in form of acceptor like electron traps and donor like traps in $HfO_2$ and $ZrO_2$ metal-oxide-semiconductor capacitors [Zhao et al, 2009]. It is expected that ionizing radiation produces structural defects in oxides (colour centres or oxygen vacancies) and variation in defect density changes upon exposure to gamma-rays [Trefilova *et al,* 2001]. These defects can be associated with impurities and occasionally due to change in cation balance or oxygen nonstoichiometry. Hence the radiation induced defects govern electronic, optical and transport properties of the material and typically dominate in respect of surface chemistry. The radiation dose and the parameters of the films decide the radiation induced damage [Atanassova *et al,* 2001]. Several efforts have been carried

out to investigate the influence of radiation on the material properties of metal oxides [Zhang *et al,* 2002]. The electrical and dielectric properties of thin tantalum pentaoxide layers in terms of dielectric constant, leakage current and oxide charge was found to degrade after gamma irradiation doses of $10^6$ - $5x10^7$ rad. The major source of electrically active defects was associated with the oxygen vacancies and the broken Ta–O and Si–O bonds in irradiated films. Surface oxidative abilities and catalytic activities changes were observed in NiO film with irradiation of 1 MGy gamma dose. Electron and gamma ray irradiation of titanium oxide films resulted in reduction $Ti^{4+}$ ions in the thin film layer.

### 2.11.1 High Energy Radiation Effects on Perovskite Oxides

Meldrum *et al* has studied effects of high energy irradiation on oxides having perovskite structure [Meldrum *et al,* 2002]. Radiation effects by irradiation of Ar ions and fast neutrons [Ball *et al,* 1988] have been studied in $CaTiO_3$. In general, perovskite $CaTiO_3$ appears to be relatively resistant against ion irradiation with respect to other actinide-bearing phases [Smith *et al,* 1999]. $CaTiO_3$ and $BaTiO_3$ were found good resistant against high energy radiation and amorphisation could not be produced by fast neutrons or 4 MeV protons, respectively while formation of oxygen interstitials gives rise to displacement damage. Interstitial-type dislocation loops during electron irradiation were confirmed to form preferentially at the ferroelectric domain walls [Buck, 1995].

The role(s) of defects on ferroelectric performance in thin films are important due to its strong impact on extrinsic properties mainly linked to the interaction of crystallographic or electronic and domain walls. Therefore it is necessary to investigate radiation induced damage accumulation to assess a device lifetime and suitability in above mentioned radiation environments. The vacancy and cluster concentrations are process independent in irradiated materials and primarily depend on radiation dose and defect reactions. Hence the microstructure plays a crucial role in damage growth and subsequent changes in material properties. It has been reported that neutron effects in PZT is roughly an order of magnitude lower damage thresholds in thin film compared to bulk [Toacsan *et al,* 2007; Miclea *et al,* 2005]. It is also anticipated that a variety of defect dipoles and other charged defects may form in irradiated PZT, providing a broader landscape of domain wall pinning sites and other possible effects on switching behavior. Much effort has been invested to study the role of mechanical and temperature stress on the degradation of ferroelectric materials while relatively little is known about the radiation induced ionization and displacement effects. The literature has focused primarily on device level properties although some inferences have been emerged out to the microscopic degradation mechanisms which are significant in radiation induced degradation. Moreover, few studies have specifically investigated damage in thin films where the effects of clustering and defect reactions may play a sensitive role.

Miclea *et al.* found that the dielectric properties changes upon neutron irradiation [Miclea *et al,* 2005]. At higher neutron fluxes relative permittivity as well as loss tangent was observed to decrease. Together these results explains that, somehow, radiation induced defects reduces the polarizability of the PZT while also diminishing loss mechanisms and similar results was reported by Toacsan *et al* [Toacsan et al, 2007]. The authors claimed that the decrease in permittivity and loss tangent evidenced oxygen vacancies as main defect, produced by neutron irradiation. It has been anticipated based on elementary damage theory where the defects exist within neutron irradiated perovskites including A, B and O site vacancies and interstitials, trapped mobile charge carriers and defect clusters. Various authors have suggested that oxygen vacancies play a dominant role while material is irradiated with high energy radiation.

Ferroelectric behavior is affected by charged defects, acting as pinning sites that hinder domain wall motion. The motion of domain wall may encounter to defects as it move under the effect of an applied field. The electric fields of charged defects result in scattered local minima and maxima in the free energy landscape of the domain wall by interaction of defects field with the polarization density in the vicinity of the domain wall. This interaction makes up the field of pinning sites in the material. Defect dipoles are formed from point defect complexes, are known

to be an important class of charged defects [Ovchinnikov *et al,* 2009]. Potential satellite and spacecraft applications of ferroelectric materials like BST & PZT include communication frequency filter and Fe-RAM in satellites. Other high radiation applications of PZT include a high intensity and energy radiation detector [Miyachi *et al,* 2002] for use in reactor application. There are two types of oxygen vacancies and observed that the $VO_1$ vacancy is energetically more stable [Park and Chadi, 1998] than the $VO_2$ vacancy due to increased tetragonal lattice strain energy at the $O_2$ sites. The vacancies are produced through knock-on reactions and there is no preference for the type of O vacancies produced. In addition domain wall pinning from polar defect clusters, local lattice deformation and charged defects could be accountable for changes in the properties. The domain structure was analysed and observed depolarized and deformed grains as well as randomly oriented domains of irradiated PZT. These processes involve inhibition of domain wall pinning and domain nucleation sites. Domain wall motion contributes significantly to the ferroelectric properties of the material while domain wall pinning is an important process because of structural and charged defects. Moore *et al* studied neutron effects in thin film capacitors and showed direct applicability of memory devices for space and neutron environments [Moore *et al,* 1991]. It has been indicated that the decrease in remnant polarization can be attributed by three possible reasons i.e. defect clusters nucleate reverse domains, defect clusters act as domain wall pinning sites and neutron induced space charges polarization.

Several studies have been carried out for the total dose effects of gamma rays on dielectric oxides. Gamma irradiations carry change primarily through ionizations and isolated Frenkel pairs. Intercation of ionizing radiation gives rise to generation of a large amount of electron-hole pairs. Electric fields within the material give separation to these mobile charges. The average displacement and local electric fields, coupled with the bulk of domains are excessively weak to separate charges appreciably. However, strong localized fields taking place near structural discontinuities like grain boundaries and ferroelectric-electrode interfaces, separate charges to create space charge. The accumulated space charge should enhance with the total gamma dose and the rate of accumulation is likely to depend on the total grain boundary area. With assumption of charge trapping at grain boundaries, trapping will be increased with increasing grain boundaries. The trapped charges form dipole-like local electric field which contribute to the depolarization and hence distorts the hysteresis curve. Lee *et al* observed loss of remnant polarization and the presence of an internal bias field upon irradiation which narrows and shifts downward upon irradiation with a $^{60}Co$ source [Lee *et al,* 1992]. Similar distortions to those observed in the Lee *et al.* study have been revealed by Benedetto *et al.* with irradiation from 10 keV x-rays using sol-gel derived capacitors [Benedetto *et al*, 1990]. With increased dose up to 100 Mrad, a buildup of internal bias and a reduction in the remnant polarization as evidence of charge trapping at the grain boundaries. Unlike gamma irradiation, neutron irradiation does appear to degrade the retention properties. Interestingly, with increasing number of cycles the Benedetto *et al.* observed an increase in remnant polarization while Lee *et al.* observed a decrease. These results might indicate more susceptible of Benedetto films to increased leakage upon irradiation. Gao *et al* [Gao *et al,* 1999] observed similar behavior in the internal bias field of irradiated thin film capacitor to that seen in the studies by Lee *et al.* and Benedetto *et al.* They attributed their results by charge trapping at the grain boundaries which are highly dense in thin films and found remnant polarization to increase with dose. This increase in polarization was interpreted with buildup of space charge around the grain boundaries which magnifies the depolarization field.